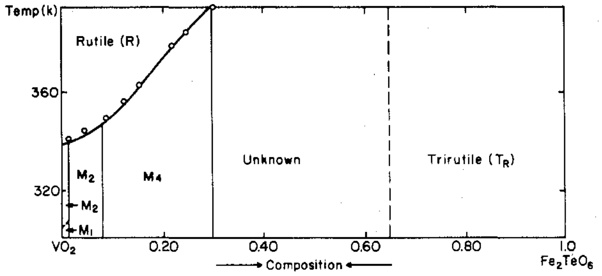

Figure 4. Phase diagram for $V_{1-x}Fe_{2x/3}Te_{x/3}O_2$.

$AlVO_4$-substituted VO_2 at ~354 K.

High-temperature x-ray results show that the rutile (R) structure forms in all of the compositions above the T_{tr}. In the particular compositions where $0 \leq x \leq 0.015$, a sequence $M_1 \rightarrow M_2 \rightarrow R$ has been reported with increasing temperature. The $M_1 \rightarrow M_2$ transition is indicated by a dotted line in Figures 2–4. Precise DTA and x-ray work is needed to characterize the $M_1 \rightarrow M_2$ transition temperature, since it lies close to room temperature.

The overall effect of composition on T_{tr} has been surveyed in other rather comprehensive investigations.[9,11,12,15–17] It appears that cations with ionic radii smaller than that of V^{4+} shift the T_{tr} toward higher temperatures, and vice versa. It is interesting to note that the present results follow this trend for smaller (e.g., Al + Te, Cr + Te, Cr + V, Ge^{4+}, etc.) and larger ($V^{3+} + W^{6+}$, Mo^{4+}, Nb^{4+}, etc.) cations, but they hold poorly for cations ($Cr^{3+} + Mo^{6+}$, $Cr^{6+} + W^{6+}$, $Fe^{3+} + Te^{6+}$) having mean ionic radii close to but slightly higher than that of V^{4+}. Although the results of the $V_{1-x}Cr_{2x/3}M_{x/3}O_2$, M = W or Mo, solid solution[3] are not sufficient to generalize, it was tentatively suggested that the character of each ion should be considered separately, where more than one ion is introduced for V^{4+}. The DTA measurements on $V_{1-x}Fe_{2x/3}Te_{x/3}O_2$ solid solution clearly signify that both Fe^{3+} and Te^{6+} support the T_{tr} shift toward a higher temperature. There exists, however, a controversy on Fe^{3+} substitutions on the transition temperature of VO_2. Futaki and Aoki[12] claimed that when Fe^{3+} was added to VO_2 the T_{tr} shifted to a lower temperature. According to the results obtained by McChensney and Everhart[10] the T_{tr} shifts toward a higher temperature for Fe^{3+}-doped VO_2. The present work as well as our unpublished data on the system $V_{1-2x}Fe_xNb_xO_2$[18] favors the T_{tr} shift toward higher temperatures.

Hence, in surveying all of the experimental results reported on VO_2–$M^{III}{}_2M^{VI}O_2$ systems to date, it is remarkable that the structural changes can be predicted so consistently on the basis of ionic size, but no consensus has yet been reached concerning the mechanism responsible for the transition in VO_2.

Acknowledgment. The authors extend their thanks to Professor I. R. Harrison for providing the DTA facilities for this work.

References and Notes

(1) J. C. Bernier and P. Poix, *C. R. Hebd. Seances Acad. Sci., Ser. C*, **265**, 1247 (1967).
(2) A. Bernigaud, J. C. Bernier, and A. Michel, *Rev. Int. Hautes Temp. Refract.*, **8**, 261–268 (1971).
(3) R. R. Neurgaonkar and R. Roy, *Mater. Res. Bull.*, **11**, 361–368 (1976).
(4) G. Villeneuve, A. Bordet, A. Casalot, and P. Hagenmuller, *Mater. Res. Bull.*, **6**, 119–130 (1971).
(5) M. Marezio, D. B. McWhan, J. P. Remeika, and J. P. Dernier, *Phys. Rev. B*, **5**, 2541–2551 (1972).
(6) G. Villeneuve, M. Drillon, and P. Hagenmuller, *Mater. Res. Bull.*, **8**, 1111–1122 (1973).
(7) J. Galy, A. Casalot, J. Darriet, and P. Hagenmuller, *Bull. Soc. Chim. Fr.*, 223 (1967).
(8) K. Kosuge, *J. Phys. Soc. Jpn.*, **22**, 551 (1967).
(9) T. Mitsuishi, *Jpn. J. Appl. Phys.*, **6**, 1060 (1967).
(10) C. R. Everhart and J. B. McChensney, *J. Appl. Phys.*, **39**, 2872 (1968).
(11) J. Umeda, S. Ashida, M. Kusumoto, and K. Narita, *J. Phys. Soc. Jpn.*, **21**, 1461 (1966).
(12) H. Futaki and M. Aoki, *Jpn. J. Appl. Phys.*, **8**, 1008–1013 (1969).
(13) J. Kitahiro and A. Watanabe, *Jpn. J. Appl. Phys.*, **6**, 1023–1024 (1967).
(14) M. Drillon and G. Villeneuve, *Mater. Res. Bull.*, **8**, 1199–1208 (1974).
(15) J. B. McChensney and H. J. Guggenheim, *J. Phys. Chem. Solids*, **30**, 225–234 (1969).
(16) J. Umeda, H. Kusumoto, K. Narita, and E. Yamada, *J. Chem. Phys.*, **42**, 1461 (1965).
(17) J. B. Goodenough, *J. Solid State Chem.*, **3**, 490–500 (1971).
(18) R. R. Neurgaonkar and R. Roy, submitted for publication.
(19) Ionic radii used in the present classification are taken from the work R. D. Shannon and C. T. Prewitt, *Acta Crystallogr., Sect. B*, **25**, 925 (1969); **26**, 1046 (1970).

Contribution from the Institute of Scientific and Industrial Research,
Osaka University, Suita, Osaka 565, Japan

Synthesis and Characterization of the Organic Derivatives of Zirconium Phosphate[1]

SHOJI YAMANAKA[2]

Received March 4, 1976 AIC60164Y

When γ-zirconium phosphate is immersed in an aqueous solution of ethylene oxide, it is converted into new phases with enlarged basal spacings. Unlike usual intercalated complexes, the resulting phases are very stable to heating up to about 200 °C and to washing with various solvents. In alkaline solution, they are hydrolyzed into the phosphoric ester of ethylene glycol and zirconium hydroxide gel. Analysis by infrared spectroscopy and hydration studies on the new phases indicate that ethylene oxide is not merely adsorbed but suffers ring scission upon reaction with the phosphate groups on the interlamellar surfaces of γ-zirconium phosphate. The amount of reacted ethylene oxide and the basal spacing of the organic derivative vary depending upon the reaction conditions, and there is a linear relation between the two. A possible structural model for the organic derivative is proposed on the basis of this linear relation.

Introduction

Many inorganic substances with a layered structure form intercalated complexes with polar organic molecules. Such complexes have been reported on clay minerals,[3–5] transition metal chalcogenides,[6,7] hydroxy salts,[8,9] iron(III) oxychloride[10] and others.[11] In most of these complexes adsorbed species are loosely bound to the host layers and are easily removed by evacuation or may be exchanged with other polar molecules, such as water in the atmosphere. If adsorbed molecules were linked by a covalent bond to the interlamellar surfaces, however, more stable complexes would be formed. These are considered to belong to the class of organic derivatives rather than to the class of sorption complexes of layer crystals. In the organic derivatives, the interlamellar surfaces as well as the outer surfaces of the layer crystals react with organic molecules. Therefore, they are considered as organic derivatives of inorganic sheet polymers or as grafting products of organic chains onto inorganic sheet polymers.

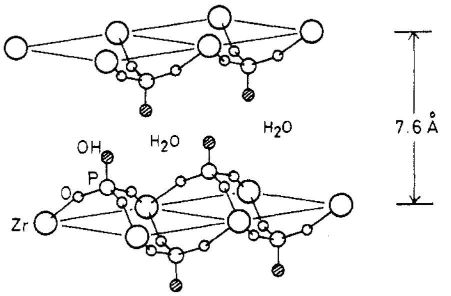

Figure 1. Schematic diagram of a portion of the structure of α-zirconium phosphate as in ref 15.

So far only a few investigators have attempted to synthesize such organic derivatives,[12] but they have not succeeded in establishing the formation of covalent bonds in the derivatives. The main objective of the present research is to synthesize examples of the above organic derivatives to ascertain that true covalent bonds are formed between interlamellar surfaces and adsorbed molecules. For this purpose, crystalline zirconium bis(monohydrogen orthophosphate), $Zr(HPO_4)_2$, hereafter called zirconium phosphate or ZrP, was selected as a host matrix because the structure of ZrP seems to be favorable for the formation of the organic derivatives.

Structural Aspects of Zirconium Phosphate

The crystal structure of α-ZrP, $Zr(HPO_4)_2 \cdot H_2O$, was determined to be layered by Clearfield and Smith[13] using single crystal techniques. A diagram of a portion of the structure is shown in Figure 1. The zirconium atoms lie very nearly on a plane and form hexagonal arrays within the plane, phosphate groups being situated above and below each zirconium layer. Three of the phosphate oxygens are bound to three different zirconium atoms; the fourth oxygen bears a hydrogen atom and points toward an adjacent plane. It should be possible to make use of these interlamellar $\equiv$P—OH groups for the esterification reaction to form a P–O–C linkage because, as described in a previous paper,[14] various organic molecules can penetrate into the interlayer regions of ZrP.

Several other forms of ZrP have been reported[15,16] which differ in the method linking the layers together and in the influence of interlayer water of hydration. For instance, the γ form has a composition $Zr(HPO_4)_2 \cdot 2H_2O$ and the basal spacing is 12.3 Å. The proposed structure has a greater interlayer spacing than that of α-ZrP allowing adsorption of more kinds of organic molecules.[14] In the present study, the phosphate groups of the interlamellar surfaces of α- and γ-ZrP have been esterified through reaction with ethylene oxide.

Experimental Section

Host Layers. α-Zirconium phosphate was prepared by the method of Clearfield and Stynes[17] by refluxing ZrP gel in 10 M phosphoric acid for 50 h. The γ form of ZrP was prepared according to the method reported by Clearfield et al.[15] The procedure was modified as follows: $ZrOCl_2 \cdot 8H_2O$ solution (100 ml, 1 M) was added dropwise to a constantly stirred, refluxing hydrochloric acid solution of NaH_2PO_4 (200 g of $NaH_2PO_4 \cdot 2H_2O$ in 200 ml of 2 N HCl). The zirconium phosphate gel, which precipitated immediately, was refluxed in its mother liquor for 3 h and then the gel was sealed in Pyrex glass tubes with its mother liquor. The tubes were heated for several days at 180 to 190 °C in an autoclave. The resulting crystalline zirconium phosphate was filtered off and washed with 2 N HCl to remove sodium ions (several liters were required) and then with distilled water until free from chloride ions. The product was dried at 35 °C in air. Chemical analysis of γ-ZrP was carried out by the method reported by Clearfield and Stynes.[17] The analytical result revealed that the γ-ZrP prepared had a stoichiometric composition, $Zr(HPO_4)_2 \cdot 2H_2O$, as reported by Clearfield et al.[15]

Reagents. Ethylene oxide was prepared from ethylene chlorohydrin by eliminating hydrogen chloride with NaOH. It was purified by distillation and a known amount was dissolved in distilled water. Standard materials for thin-layer chromatography were prepared as follows: barium bis(2-oxo-1,3,2-dioxaphospholane 2-oxylate) ($Ba[C_2H_4PO_4]_2$, or barium ethylene phosphate) was synthesized from barium mono(2-bromoethyl) phosphate according to the procedure developed by Kumamoto et al.[18] The ^1H NMR spectrum of the barium ethylene phosphate in D_2O as solvent showed a doublet at 0.41 ppm, relative to water, and J_{H-P} was 11 Hz, consistent with the data reported for barium ethylene phosphate.[18] Barium mono(2-hydroxyethyl) phosphate ($Ba[HOC_2H_4PO_4]$, or barium ethylene glycol phosphate) was prepared by hydrolysis of barium ethylene phosphate[19] and was also synthesized from ethylene oxide and disodium hydrogen phosphate followed by precipitation as the barium salt.[20] Barium mono[2-(2-hydroxyethoxy)ethyl] phosphate ($Ba[HOC_2H_4OC_2H_4PO_4]$, or barium diethylene glycol phosphate) was prepared by the reaction of pyrophosphoric acid and diethylene glycol. The desired barium salt precipitated from an aqueous ethanol after removing barium phosphate by addition of barium hydroxide.[21]

A weighed amount of each barium salt was dissolved in water and treated with a solution containing a calculated quantity of sodium sulfate. Precipitated barium sulfate was removed by centrifugation, and the supernatant liquid was used as a standard for thin-layer chromatography.

General Procedure. X-ray examination was carried out on a Rigaku-denki diffractometer using Ni-filtered Cu Kα radiation. Infrared absorption spectra were obtained on a Hitachi Perkin-Elmer EPI-2G spectrometer. Differential thermogravimetric analysis was made up to 1000 °C using a Rigaku-denki unit programed for a heating rate of 10 °C/min. Gas chromatographic analysis was performed on a Shimazu gas chromatograph GC-3BT using a 3 mm × 1.3 m column of 20% polyethylene glycol 20M on 60–80 mesh Shimarite at 155 °C. The sorption isotherms of water on the γ-ZrP that reacted with ethylene oxide were measured using a quartz spring balance. ^1H NMR spectra were recorded at 100 MHz in D_2O solutions on a JEOL JNM-MN-100 spectrometer. Potentiometric titrations were carried out using a potentiometer Model HM-5A made by Toa Electronics. Thin-layer chromatograms were run on Funakoshi-Cellulose plates. The solvent for the development was prepared by mixing 25 ml of ethyl alcohol, 7.5 ml of concentrated NH_3, 15 ml of water, and 25 mg of trichloroacetic acid. The plates were dried in air at 80 °C after the development, sprayed with Hanes and Isherwood reagent,[22] and then dried again at 80 °C. The spots were colored by exposing the plates to ultraviolet light.[23]

Reaction of γ-ZrP with Ethylene Oxide. Separate samples of 0.3 g of γ-ZrP were dispersed in 50 ml of ethylene oxide aqueous solutions ranging in concentration from 0.5 to 5 M and closed in glass tubes with tapered rubber plugs. After various intervals of reaction under occasional shaking of the solutions in a water bath thermostated at temperatures below 30 °C, the glass tubes were withdrawn out of the bath and the reaction was quenched by diluting the ethylene oxide solutions with 500 ml of distilled water. Then, the reaction products were separated by filtration. The filtration was carried out using Sartorius membrane filter MF125 to prevent contamination with filter paper. The separated solid was washed with excess distilled water (200 ml), air-dried for 1 day at 40 °C, and finally equilibrated with air of 70% humidity.

Reaction of α-ZrP with Ethylene Oxide. Since α-ZrP did not react wih ethylene oxide under the condition used in the case of γ-ZrP, the reaction was carried out at elevated temperatures. α-ZrP and liquid ethylene oxide were heated for 3 days in an autoclave at 70 °C. The phosphate which was covered with a syrupy liquid which might be polymerized ethylene oxide was recovered by dispersion in excess water followed by filtration, washing with water, and air-drying.

Hydrolysis of the Reaction Product of γ-ZrP. About 10 g of γ-ZrP was dispersed in 500 ml of 3 M ethylene oxide solution for 20 h at 25 °C and then separated by filtration followed by washing with distilled water. The resulting product was dried in air at 40 °C for 1 day and supplied for the hydrolysis study. The product is denoted hereafter as ZrP·2EO, since the analysis of this product revealed that 2.0 mol of ethylene oxide was reacted per mol of $Zr(HPO_4)_2$. Separate samples of 100 mg of ZrP·2EO were added into 30 ml of 1 N NaOH and 30 ml of 1 N HCl solutions and heated at 70 °C for 1 h. Then, the remaining solids were separated by filtration, washed with distilled water until free from Na and Cl ions, respectively, and air-dried. The alkaline filtrate was neutralized with 3 N HCl and condensed by evacuation at 70 °C and supplied for the analysis by cellulose thin-layer chromatography.

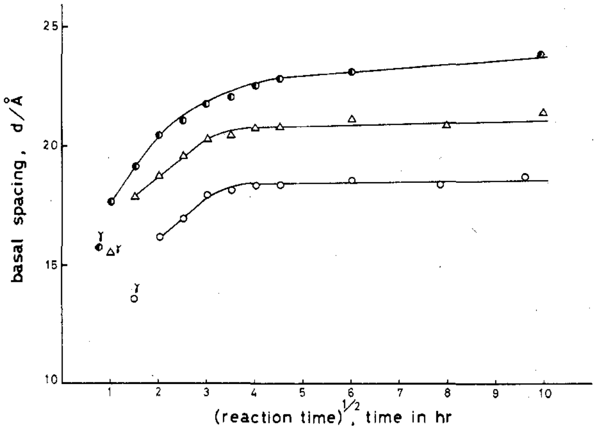

Figure 2. Basal spacings of the reaction products at various stages during the reaction in ethylene oxide solutions in the concentration of 1 M (○), 3 M (△), and 5 M (◐) at 30 °C. A part of γ-ZrP remained unreacted at the reaction stages indicated with γ.

Isolation of Phosphoric Esters from the HF Solution of ZrP·2EO. About 4 g of ZrP·2EO was dissolved in a HF solution (2–3 ml of concentrated HF in 15 ml of water). Soon after complete dissolution, the solution was diluted to 50 ml with distilled water in a polyethylene beaker and rapidly neutralized with a saturated barium hydroxide solution against an outer indicator of phenolphthalein. The precipitate was filtered off and rinsed three times with 50 ml of water. The filtrate together with the rinse water was evaporated to a syrup at 70 °C and 20 Torr. The syrup was dissolved in 10 ml of water, and 50 ml of absolute alcohol was added into the solution. Crystals of barium ethylene glycol phosphate formed during the next 3 h were removed by filtration and discarded. The filtrate was evaporated again to a syrup at 70 °C, and the above procedure was repeated twice to remove barium ethylene glycol phosphate more completely. The syrup obtained after a final evaporation was very viscous just like water glass and hygroscopic and did not crystallize even when it was evacuated under a pressure of 10^{-3} Torr for 1 day.

Results and Discussion

X-Ray Diffraction Study. X-ray diffraction analysis of the product of γ-ZrP with ethylene oxide revealed that the reflections due to γ-ZrP were broadened and reduced in intensity at the first stage of the reaction. Then, a new reflection appeared at lower diffraction angle than any other reflections of γ-ZrP. As the reaction proceeded, reflections due to the basal spacing of γ-ZrP disappeared and the position for the new reflection was shifted toward lower diffraction angles. The increase in the *d* value for the new reflection in the course of the reaction of γ-ZrP in ethylene oxide solutions of the concentrations 1, 3, and 5 M is shown in Figure 2. Although the products with enlarged basal spacing had less crystallinity in comparison with the starting γ-ZrP, some integral reflections corresponding to the higher orders of the enlarged basal spacing were observed. The appearance of the enlarged spacing seems to be due to the intercalation of ethylene oxide.

The change in basal spacing shown in Figure 2 is a representative case. The reaction products had different values of basal spacings depending upon reaction conditions: the higher the concentration of ethylene oxide solution and reaction temperature, the larger the basal spacing of the product. The crystallinity and the particle size of γ-ZrP also seemed to affect the spacing. However, the reaction product with a basal spacing of 18.4 Å was obtained especially when γ-ZrP was reacted with ethylene oxide solutions of concentrations lower than 3 M and below 20 °C.

The amount of ethylene oxide that reacted with 1 mol of $Zr(HPO_4)_2$ was determined on the basis of weight loss data obtained by thermogravimetric analysis. The amount of ethylene oxide obtained in the above way for each reaction product whose basal spacing was given in Figure 2 is indicated in Figure 3. The details of the calculation are described later in this paper. It is noted that the amount of the reacted ethylene oxide increases almost linearly with the square root of the reaction time before the uptake of ethylene oxide ceases. This finding suggests that the reaction proceeds through the diffusion of ethylene oxide into the interlayer spaces.[24]

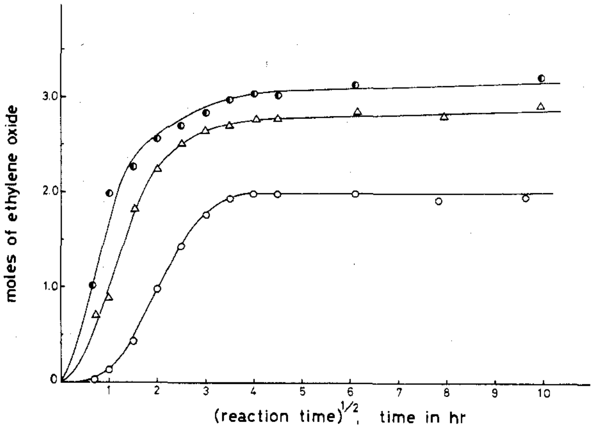

Figure 3. The amount of ethylene oxide contained in the reaction products at various stages during the reaction in ethylene oxide solutions in the concentration of 1 M (○), 3 M (△), and 5 M (◐) at 30 °C. The number of moles of ethylene oxide per mole of $Zr(HPO_4)_2$ is plotted against $(\text{reaction time})^{1/2}$.

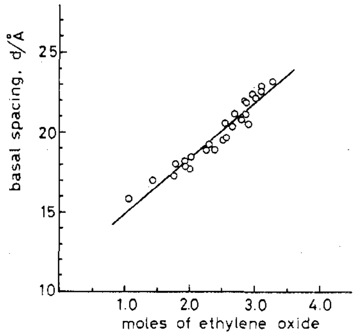

Figure 4. Linear relation between the amount of ethylene oxide in the reaction products and basal spacings.

Though various basal spacing values were obtained, they can be related to the amount of reacted ethylene oxide by a linear relation as illustrated in Figure 4. The implication of the linear relationship is discussed later in relation to the structure of the reaction product of γ-ZrP.

Differing from usual sorption complexes, the products were very stable against washing with water and with polar organic solvents such as alcohols and acetone and moreover do not lose the ethylene oxide when heated at 180 °C for 2 days. It is not possible to explain the reaction of γ-ZrP with ethylene oxide as the formation of a sorption complex such as a γ-ZrP–ethylene glycol complex because, although ethylene oxide reacts with water to form ethylene glycol in the presence of an acidic catalyst, and γ-ZrP forms a complex having a basal spacing 13.4 Å upon reaction with ethylene glycol,[14] the complex easily reverts to the initial γ-ZrP only by washing with water, losing the adsorbed ethylene glycol. These findings lead to the conclusion that ethylene oxide is not merely adsorbed but reacts with the phosphate groups of the interlamellar surfaces to form an organic derivative of γ-ZrP.

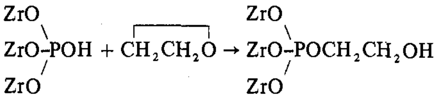

$$\mathrm{(ZrO)_3POH + \overline{CH_2CH_2O} \rightarrow (ZrO)_3POCH_2CH_2OH}$$

It is noteworthy that this reaction is very analogous to the well-known one:[20]

$$\mathrm{Na_2HPO_4 + \overline{CH_2CH_2O} \rightarrow Na_2(HOCH_2CH_2OPO_3)}$$

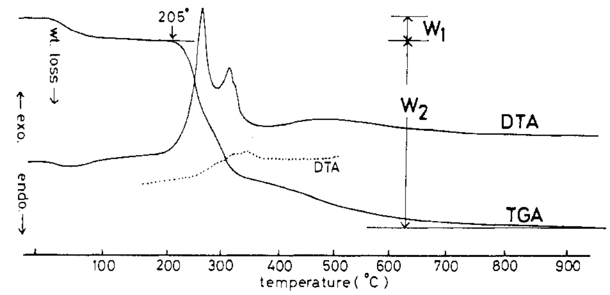

Figure 5. Thermal analysis curves for the reaction products of γ-ZrP containing 2.95 mol of ethylene oxide per mol of $Zr(HPO_4)_2$. Dotted DTA curve was recorded in an atmosphere of nitrogen.

The latter reaction proceeds in a homogeneous system, for Na_2HPO_4 and ethylene oxide are soluble in water. On the other hand, in the case of the reaction under investigation, γ-ZrP is not soluble, and therefore ethylene oxide intercalates into the interlayer spaces, expanding the basal spacing and reacting with phosphate groups of the interlamellar surfaces.

Thermogravimetric analysis of the above-mentioned product with a basal spacing of 18.4 Å revealed that just 2 mol of ethylene oxide had reacted with 1 mol of $Zr(HPO_4)_2$. Since 1 mol of ZrP contains 2 mol of phosphate groups, all the phosphate groups must have reacted with ethylene oxide in this product according to the following equation:

$$Zr(HPO_4)_2 + 2\ \overline{CH_2CH_2O} \rightarrow Zr(HOCH_2CH_2OPO_3)_2$$

α-ZrP did not react with ethylene oxide as easily as γ-ZrP. The x-ray diffraction patterns of the reacted α-ZrP showed an asymmetric broadened peak with a maximum at the *d* spacing ranging from 19 to 21 Å, indicating successive stages of reaction. The greater ease of the reaction can be explained in terms of the more open structure of γ-ZrP.

Further characterizations were carried out on the reaction product of γ-ZrP. Data described below also provide powerful evidence to confirm the formation of the P–O–C ester bond on the interlamellar surfaces.

Thermal Analysis. Representative curves of differential thermal analysis and weight loss for the reaction product of γ-ZrP are shown in Figure 5. Regardless of the amount of uptake of ethylene oxide, all the thermograms exhibit a pattern similar to that shown in Figure 5. The first weight loss accompanied by an endothermic peak around 60 °C can be assigned to the loss of adsorbed water. The amount of the water varies according to the drying conditions used for the sample. The second weight loss begins at 205 °C, and finally the sample converts into a cubic phase which is identified as ZrP_2O_7 from the x-ray diffraction data.[25] This phase is identical with that obtained by heating γ-ZrP to 1000 °C. Therefore, the weight losses observed subsequent to the dehydration of adsorbed water can be attributed to the decomposition of organic species and to dehydration accompanied by the formation of ZrP_2O_7.

The amount of uptake of ethylene oxide (*n* mol) per mol of $Zr(HPO_4)_2$ is calculated using the following equation:

$$\frac{44n + 18}{44n + 283} = \frac{W_2}{W_0 - W_1}$$

where W_0 is the weighed amount of the sample for the measurement; W_1 is the first weight loss due to adsorbed water; W_2 is the second weight loss; and the constants of 44, 18, and 283 are the molecular weights of ethylene oxide, water, and $Zr(HPO_4)_2$, respectively.

When the thermal analysis was performed under nitrogen gas flow the decomposition temperature was not shifted but the vigorous exothermic peaks which had appeared near the decomposition temperature were markedly reduced as shown in Figure 5 by a dotted line. This indicates that the exothermic peaks were due to an oxidation of the decomposition products of the sample.

Infrared Spectra. The infrared spectra of the γ-ZrP reacted with ethylene oxide resembled very much that of barium ethylene glycol phosphate in the region of 4000 to 1200 cm^{-1}, and absorption bands due to ethylene oxide were not observed; the broad band with the absorption maximum at 3350 cm^{-1} was assigned to the hydrogen bonded OH stretching vibration of the C–O–H groups. The band due to adsorbed water was observed at 1630 cm^{-1}, and the intensity of this absorption changed according to the extent of dehydration. The bands at 2945, 2880, and 1457 cm^{-1} can be attributed to the vibrations of CH_2 groups. Since absorption bands which appeared in the region 1200 to 900 cm^{-1} were too intense, the spectrum in this region was measured separately on a sample with a decreased thickness. The initial γ-ZrP showed two absorption bands due to $HOPO_3^{2-}$ groups in this region: a shoulder band at 1070 cm^{-1} and an intense band at 1020 cm^{-1}. As the reaction of γ-ZrP with ethylene oxide proceeded, these two bands of γ-ZrP disappeared and new absorption bands appeared at 1137, 1030, and 1000 cm^{-1}. It is well known that materials containing the P–O–CH_2– groups give absorptions in the range 1170 to 1140 cm^{-1} accompanied by the band at 1030 cm^{-1}, which is characteristic of the C–O–P link.[26] Therefore, the appearance of absorption at 1137 cm^{-1} accompanied by the band at 1030 cm^{-1} was also attributed to the presence of P–O–C linkage.

Hydrolysis of ZrP·2EO. Pure γ-ZrP can act as an inorganic ion exchanger. It may exchange interlayer protons with Na cations in NaOH solution, and the Na form reversibly changes into the initial γ-ZrP on washing with HCl solution. On the other hand, ZrP·2EO was easily hydrolyzed in 1 N NaOH solution at 70 °C and changed into a gel, but it was stable in acidic solution of 1 N HCl at 70 °C. The hydrolysis of ZrP·2EO was completed within several minutes even when it was added to 1 N NaOH solution at room temperature. The resulting gel formed by the hydrolysis of ZrP·2EO in 1 N NaOH was converted to the tetragonal phase of ZrO_2, accompanied by about 35% weight loss due to dehydration on heating to 900 °C. The degree of hydrolysis was nearly complete as determined by comparing the ZrO_2 formed with ZrP_2O_7 obtained by burning ZrP·2EO. On prolonged heating above 1000 °C, the tetragonal ZrO_2 converted into the monoclinic form of ZrO_2, which is a more stable form of ZrO_2 at room temperature.

It is well known that a small amount of impurity such as hydroxyl and chloride ions effects the conversion of tetragonal ZrO_2 metastable at room temperature[27,28] to the monoclinic form in the temperature region of 400 to 600 °C. In the zirconium hydroxide gel prepared through the hydrolysis of ZrP·2EO, trace amounts of phosphate groups, as a result of incomplete hydrolysis, remained as an impurity to enhance formation of tetragonal ZrO_2. It is noteworthy that the tetragonal ZrO_2 obtained by hydrolysis of ZrP·2EO has an unusually high transition temperature. Further study on this tetragonal ZrO_2 will be published elsewhere.

The alkaline solution from which zirconium hydroxide gel was separated by filtration was neutralized and analyzed by cellulose thin-layer chromatography. The chromatogram indicated the presence of ethylene glycol phosphate and orthophosphate ions at the positions of R_f 0.46 and 0.25, respectively. The presence of orthophosphate ions seems to be due to a partial hydrolysis of ethylene glycol phosphate in NaOH solution. Besides the above two spots, another spot was observed at R_f 0.84. However, this spot did not correspond to any of the spots used as standards, though it was located

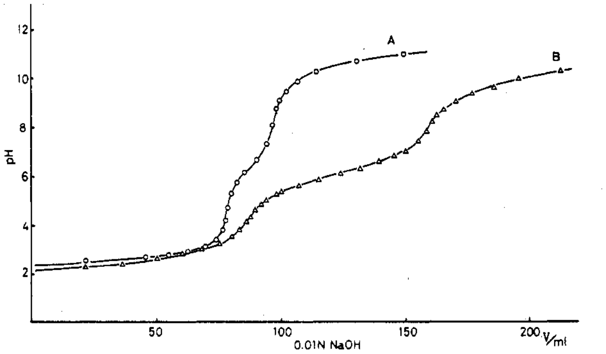

Figure 6. Potentiometric titration curves of the compound I: (A) first titration curve; (B) second titration curve after hydrolysis.

near the spot for sodium ethylene phosphate at R_f 0.80. This unidentified material (I) could also be isolated from the hydrofluoric acid solution of ZrP·2EO as a viscous hygroscopic barium salt. Details of the isolation procedure are described in the Experimental Section. Although the R_f value for I was very close to that of barium ethylene phosphate, the ^{1}H NMR spectrum of the former in D_2O did not show a doublet characteristic of barium ethylene phosphate[18] but was very similar to that of barium ethylene glycol phosphate: the τ values relative to water for barium ethylene glycol phosphate are 0.86, 0.97, and 0.99 and those for I are 0.89, 0.97, and 0.99.

Aliquots of I were passed through the hydrogen form of Amberlite CG120I to remove barium ions, and the eluate was potentiometrically titrated with 0.01 N NaOH solution.[29] The titration curve exhibited two inflection points near pH 5 and 9 as shown in Figure 6, indicating the presence of two kinds of ionization constants just like the primary ester of phosphoric acid,[29] whereas ethylene phosphate, a secondary ester, showed only one inflection point at pH 7. These results indicate that I was not barium ethylene phosphate.

After the titration with NaOH solution, the pH of the titrated solution was again brought to about 2 by adding HCl. The sample was heated on a water bath for 3 h and then cooled to room temperature. The solution was titrated again with the NaOH solution from the same batch as that used in the first titration. In the second titration curve which is shown in Figure 6, two inflection points were also observed; however, the amount of the alkali consumed in the titration between the two inflection points was about four times as much as that required for the first titration. The thin-layer analysis of the solution in the second titration with NaOH after heating with HCl revealed that the spot due to I diminished, and on the contrary a spot due to sodium ethylene glycol phosphate appeared. These results can be interpreted as follows: the unidentified material I obtained by the hydrolysis of ZrP·2EO is a condensed product of ethylene glycol phosphate, and the number-average number of phosphorus atoms per chain is approximately 4.

These results of the hydrolysis study of ZrP·2EO support the formation of the P–O–C ester bond onto the interlamellar surfaces of γ-ZrP. All related reactions presented in this section are summarized in Scheme I.

Hydration Study of ZrP·2EO. As mentioned earlier, the thermogravimetric analysis of γ-ZrP·2EO revealed that it contained adsorbed water, the amount of which varied depending upon the drying conditions. γ-ZrP·2EO, equilibrated with air (25 °C, 70% humidity), contained almost 1 mol of water per mol of $Zr(HPO_4)_2$.

Unlike the initial γ-ZrP, γ-ZrP treated with ethylene oxide solutions swelled remarkably in water and had various basal spacings. For instance, when a phase ZrP·2EO with a basal spacing 18.4 Å was subjected to swelling in water and then

Scheme I

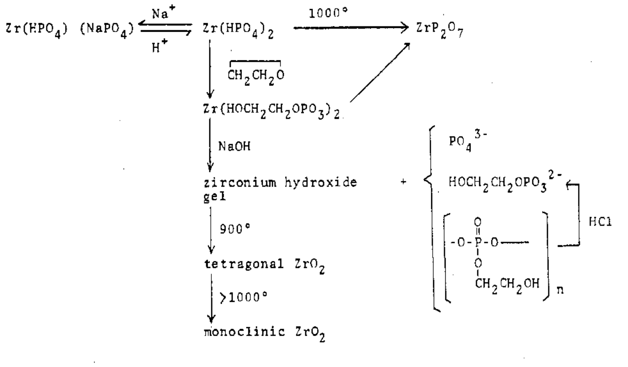

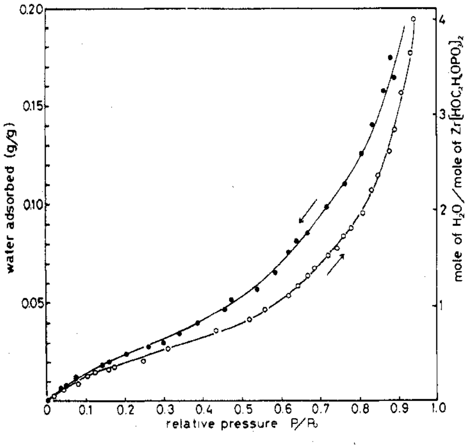

Figure 7. Adsorption–desorption isotherm of water on the reaction product of γ-ZrP containing 2 mol of ethylene oxide per mol of $Zr(HPO_4)_2$: (○) adsorption; (●) desorption.

allowed to evaporate, it showed various x-ray reflection peaks during drying: 23.9, 21.5, 20.8, 19.6, and finally 18.4 Å. When the 18.4 Å phase was further dried at 150 °C for 1 h, it changed into a new phase with a basal spacing 17.2 Å. It reverted rapidly to the 18.4 Å phase by readsorbing moisture in air.

An isothermal adsorption–desorption curve for water determined gravimetrically on the sample ZrP·2EO is shown in Figure 7. Though the basal spacing value cannot be related to the amount of adsorbed water at the present stage of this study, it is obvious that the various basal spacings arise from the intercalation of water into the interlayer spaces of the reacted γ-ZrP.

The hydration study presents another important piece of evidence that ethylene oxide reacts with the interlayer phosphate groups because if not the initial γ-ZrP instead of a 18.4 Å phase would be obtained by dehydration of ZrP·2EO swelled in water.

Gas Chromatographic Study. The P–O–C ester bond formed on the interlamellar surfaces of several products of γ-ZrP with ethylene oxide was hydrolyzed in a HF–HCl solution (1 ml of concentrated HF, 20 ml of 3 N HCl) in Teflon tubes followed by heating at 80 °C for 15 h. The resulting solution was neutralized by addition of NaOH, concentrated by evaporation, and used for GLC analysis. The solution obtained from the γ-ZrP reacted with less than 2 mol of ethylene oxide per mol of $Zr(HPO_4)_2$ showed only one peak at t_R = 1.3 min due to ethylene glycol, which was accompanied by a faint peak at t_R = 4.1 min due to trace amounts of diethylene glycol. On the other hand, the solution obtained from the γ-ZrP reacted with more than 2 mol of ethylene oxide showed two peaks, due to ethylene and diethylene glycols. The peak height due to diethylene glycol had a general tendency to increase relative to that due to ethylene glycol with an increase of the basal spacing of the reacted γ-ZrP.

The results of the GLC analysis are summarized as follows: In the case when more than 2 mol of ethylene oxide reacts with 1 mol of $Zr(HPO_4)_2$, the following dimerization occurs in the interlayer spaces,

$$\mathrm{Zr(HPO_4)_2} + (2+x)\overline{\mathrm{CH_2CH_2O}} \rightarrow \mathrm{Zr(HOCH_2CH_2OPO_3)_{2-x}(HOCH_2CH_2OCH_2CH_2OPO_3)_x}$$

Structural Considerations

As shown previously in Figure 4, uptake of 1 mol of ethylene oxide per mol of $Zr(HPO_4)_2$ results in an increase in the basal spacing by 3.5 Å. This increase can be explained using a linear relationship similar to one reported on layer silicate–organic complexes in which the complexes of a layer silicate with *n*-alkylammonium ions are allowed to swell with *n*-alkyl alcohols of equal number of carbon atoms to that in the alkyl chain. Lagaly and Weiss[30] reported that the basal spacings of the swelled complexes increased linearly as the number of carbon atoms in the alkyl chain increased. The basal spacing value, d, can be expressed as

$$d[\text{Å}] = (12.7 + 2.5n) \pm 1.0$$

where n is the number of carbon atoms in the alkyl chain. Since the value 2.5 Å in the equation corresponds to the

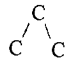

distance, 2.54 Å, they proposed a structural model for the complexes where the trans-trans alkyl chains were adsorbed in bimolecular layers in the interlayer spaces and arranged perpendicular to the silicate layers.

The slope of the straight line in Figure 4 can be interpreted in the same way in terms of the conformation of the organic chains. The slope 3.5 Å per mol of ethylene oxide is in good agreement with the oxygen–oxygen distance of the trans-trans

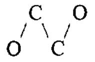

chains when they are perpendicular to the phosphate layers. This fact suggests that the arrangement of the organic chains in the organic derivatives of γ-ZrP is very similar to that of the *n*-alkyl chains proposed by Lagaly and Weiss.[30]

The perpendicular distance between the mean plane of zirconium atoms and the oxygens at the phosphate tips is about 3.3 Å, so that the thickness of the phosphate layer in γ-ZrP is twice this distance, 6.6 Å[13]. Estimating the oxygen–oxygen distance of OH---O hydrogen bands between interlayer glycol groups as 2.8 Å, a basal spacing of 16.4 Å is estimated for the dehydrated organic derivative ZrP·2EO, which is in agreement with the observed value 17.2 Å. As mentioned previously, 17.2 Å phase changed into 18.4 Å phase having a composition $Zr(HOCH_2CH_2OPO_3)_2{\cdot}H_2O$ on standing in air for hydration. In the hydrated phase, the adsorbed water is considered to take part in the formation of hydrogen bonding networks, joining two adjacent layers as schematically shown in Figure 8.

It is noteworthy that continuous increase in the basal spacing of the γ-ZrP reacted with ethylene oxide was observed in the intermediate stages of the reaction. The continuous shift of the basal spacing is frequently observed in the course of the investigation of interstratified clay minerals.[31] It is known that peaks of x-ray reflections of a randomly interstratified mixture of minerals of A and B migrate as the relative portions of the two kinds of layer change. The position of the first diffraction maximum continuously changes in the range of the two extreme positions of the first diffraction maxima of minerals A and B. The other diffraction peaks also exhibit a shift corresponding to the separation in reciprocal space, but all the reflection peaks cannot be integral to the first reflection peak. Applying this theory to the organic derivative of γ-ZrP, it seems possible to explain the continuous increase of the basal spacing as interstratification of two extreme layers such as 18.4 and 21.9 Å. However, the x-ray diffraction patterns of the derivatives consist of integral peaks due to basal reflections, indicating that the organic derivatives of γ-ZrP do not have an interstratified structure but that all the layers in the derivative must be uniformly reacted with ethylene oxide.

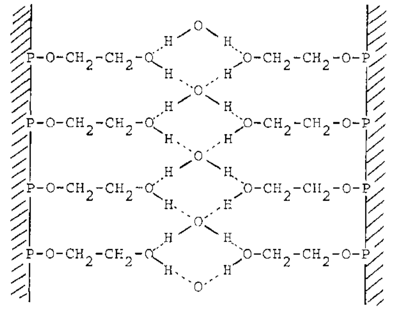

Figure 8. Schematic illustration of the arrangement of the glycol chains and water in the interlayer region of 18.4 Å phase with a composition $Zr(HOCH_2CH_2OPO_3)_2{\cdot}H_2O$.

It is a very difficult problem to explain the linear relation in the intermediate stages of the reaction of γ-ZrP with ethylene oxide. At the present stage of investigation, it is understood in terms of the formation of kinks and jogs, i.e., rotational isomers of the hydrocarbon chains containing gauche bonds.[30,32] The length of longer chains may be reduced by conformational changes from trans to gauche and the amount of the decrease in the length seems to be related to the amount of the ethylene oxide reacted with γ-ZrP. At the reaction stages where the lengths of the organic chains are uniform, the chains may be perpendicular to the phosphate layers.

In conclusion, a new type of compound was obtained when γ-ZrP was treated with ethylene oxide. All of the results obtained in the present study strongly support the formation of P–O–C ester bonds on the interlamellar surfaces of the phosphate layers. This newly synthesized material is a glycol ester of γ-ZrP. From another point of view, this is considered as an organic derivative of an inorganic sheet polymer and as such occupies a position somewhere between inorganic and organic chemistry. The present paper is not concerned with the mechanism of formation of the organic derivative. It will be published elsewhere in the future.

Acknowledgment. The author wishes to express his gratitude to Professor M. Koizumi for valuable suggestions and critical reading of the manuscript. Thanks are also due to Associate Professor F. Kanamaru for frequent and helpful discussions throughout this work. The expense of this study was partly defrayed by a Grant in Aid for Special Research Project from the Ministry of Education.

Registry No. $Zr(HPO_4)_2{\cdot}2H_2O$, 13986-21-5; ZrP·2EO, 51952-91-1; $ZrOCl_2$, 7699-43-6; ethylene oxide, 75-21-8.

References and Notes

(1) Portions of this paper were taken from the Ph.D. thesis of the author presented to Osaka University, June 1975.
(2) To whom correspondence should be addressed at the Department of Applied Chemistry, University of Osaka Prefecture, Sakai, Osaka 591, Japan.
(3) D. M. C. MacEvan, *Trans Faraday Soc.*, **44**, 349 (1948).
(4) B. K. G. Theng, "The Chemistry of Clay-Organic Reactions", Wiley, New York, N.Y., 1974.
(5) R. E. Grim, "Clay Mineralogy", McGraw-Hill, New York, N.Y., 1968, p 353.
(6) A. Weiss and R. Ruthardt, *Z. Naturforsch., B*, **24**, 355 (1969).
(7) F. R. Gamble, F. J. Disalvo, R. A. Klemm, and T. H. Geballe, *Science*, **168**, 568 (1970).
(8) J. Cano-Ruiz, D. M. C. MacEwan, and A. R. Garcia, *Nature (London)*, **205**, 696 (1965).
(9) W. Feitknecht and H. Burki, *Helv. Chim. Acta*, **39**, 589 (1956).

(10) F. Kanamaru, S. Yamanaka, M. Koizumi, and S. Nagai, *Chem. Lett.*, 373 (1974).
(11) R. M. Barrer, "Non-stoichiometric Compounds", L. Mandelcorn, Ed., Academic Press, New York, N.Y., 1964, p 309.
(12) H. Deuel, *Kolloid-Z.*, **124**, 164 (1951).
(13) A. Clearfield and G. D. Smith, *Inorg. Chem.*, **8**, 431 (1969).
(14) S. Yamanaka and M. Koizumi, *Clays Clay Miner.*, **23**, 477 (1975).
(15) A. Clearfield, R. H. Blessing, and J. A. Stynes, *J. Inorg. Nucl. Chem.*, **30**, 2249 (1968).
(16) A. Clearfield, A. L. Landis, A. S. Medina, and J. H. Troup, *J. Inorg. Nucl. Chem.*, **35**, 1099 (1973).
(17) A. Clearfield and J. A. Stynes, *J. Inorg. Nucl. Chem.*, **26**, 117 (1964).
(18) J. Kumamoto, J. R. Cox, Jr., and F. H. Westheimer, *J. Am. Chem. Soc.*, **78**, 4858 (1956).
(19) P. C. Haake and F. H. Westheimer, *J. Am. Chem. Soc.*, **83**, 1102 (1961).
(20) F. R. Atherton, H. T. Openshaw, and A R Todd, *J. Chem. Soc.*, 382 (1945).
(21) A. K Nelson and A. D. F Toy, U.S. Patent 3 146 255 (1949).
(22) C. S. Hanes and F. A. Isherwood, *Nature* (*London*), **164**, 1107 (1949).
(23) E. Karl-Kroupa, *Anal. Chem.*, **28**, 1091 (1956).
(24) P. G. Shewmon, "Diffusion in Solids", McGraw-Hill, New York, N.Y., 1963.
(25) "X-ray Powder Diffraction File", Joint Committee on Powder Diffraction Standards, Philadelphia, Pa.
(26) D. E. Corgridge, *Top. Phosphorus Chem.*, **6**, 235 (1969).
(27) E. D. Whitney, *Trans. Faraday Soc.*, **61**, 1991 (1965).
(28) A. Clearfield, *Inorg. Chem.*, **3**, 146 (1964).
(29) J. R. Van Wazer, "Phosphorus and its Compounds", Vol. 1, Interscience, New York, N.Y., 1958, pp 441, 459, and 581.
(30) G. Lagaly and A. Weiss, *Kolloid Z. Z. Polym.*, **248**, 968 (1971).
(31) D. M. C. MacEwan, A. R. Amil, and G. Brown, "The X-ray Identification and Crystal Structures of Clay Materials", G. Brown, Ed., Mineralogical Society, London, 1961, p 393.
(32) G. Lagaly and A. Weiss, *Angew. Chem., Int. Ed. Engl.*, **10**, 558 (1971).

Contribution from the Department of Chemistry,
Louisiana State University, Baton Rouge, Louisiana 70803

Absorption and Magnetic Circular Dichroism Spectra of Chromium(III) in Dicesium Sodium Yttrium Hexachloride

ROBERT W. SCHWARTZ

Received February 18, 1976 AIC60131I

The electron paramagnetic resonance, absorption, and magnetic circular dichroism spectra of Cr^{3+}:Cs_2NaYCl_6 have been measured, the latter two down to 6 K. Transitions to three doublets (^2E_g, $^2T_{1g}$, and $^2T_{2g}$) and all three quartets ($^4T_{2g}$, $^4T_{1g}$ (I and II)) were observed. The ground-state g value was 1.984 ± 0.001 and the optical spectra were fit with the parameters $F_2 = 1050$, $F_4 = 90$ ($B = 600$, $C = 3150$), $Dq = 1280$, and $\alpha = 78.2$, all in cm^{-1}. The value of ζ, the spin–orbit coupling constant, was found to vary with the electronic term. This is ascribed to varying degrees of covalency. At 6 K magnetic dipole allowed origins were observed for numerous transitions. A rich vibrational structure was also seen in many transitions at this temperature. This has been assigned effectively with the site group approximation considering only the $CrCl_6^{3-}$ moiety. A progression in an e_g vibrational mode was found in three terms but no evidence of any other Jahn–Teller effect was observed.

Introduction

As part of a continuing study of the electronic structure of metal ions at sites of undistorted O_h symmetry[1] the optical absorption, magnetic circular dichroism (MCD), and electron paramagnetic resonance (EPR) spectra of Cr^{3+}:Cs_2NaYCl_6 have been measured and are reported herein. The use of O_h symmetry simplifies theoretical considerations for d-electron systems as only one crystal field parameter, Dq, need be considered. In addition the full power of group theoretical calculations can be applied to the MCD with the least possible ambiguity. Experimentally this geometry has a simplifying effect as the fewest possible states are found; i.e., the maximum possible degeneracies still exist. The use of chloride as a ligand also aids in simplifying the observed spectrum as no strictly ligand vibrations are possible and only metal–ligand vibrations are observed. In addition this particular host lattice has the advantage that all observed transitions are well separated. Thus the problem of overlap which made any detailed interpretation of the spectrum of Cr^{3+}:K_2NaGaF_6[2] extremely difficult is eliminated.

MCD has recently been used with some success in interpreting the spectra of first-row transition metal ions.[3] In particular two studies have appeared concerning the spectrum of Cr^{3+} in octahedral (MgO[4]) and near-octahedral (potassium alum[5]) environments. The latter paper presents many general theoretical results and significant use has been made of these in the present study. A number of studies have appeared on the EPR[6] and optical spectra[7] of Cr^{3+} in octahedral or near-octahedral environments. At least one study[8] gave a detailed interpretation of the vibronic structure observed in the $^2E_g \rightarrow {}^4A_{2g}$ phosphorescence of $Cr(NH_3)_6^{3+}$. In this case the $\nu_2(e_g)$ vibration was found to be an important progression-forming mode. This also seems to be the case in the present study. The isoelectronic divalent vanadium ion has also been studied as the octahedral VF_6^{4-} species.[9] In this species a large reduction in the splitting between spin–orbit components of the lowest vibronic level of the $^4T_{2g}$ term was found. This manifestation of the Ham effect[10] might also be observed in the present case but (see below) the results are not as clearly defined.

Experimental Section

Most spectra were recorded at the University of Virginia using equipment and technique previously described.[1a,b] Spectral slit widths (shown on each spectrum) were narrow enough to eliminate any machine broadening. The samples used were checked for depolarization and strain (zero-field CD) and neither of these proved to be a problem. Temperature dependence of the MCD showed the spectrum to be composed mostly of c_0 terms.[11] In the spin-forbidden transitions (the expected sign) a_1 terms were in many cases resolved upon heating. Some temperature- and field-dependence data for the spin-allowed transitions were recorded using an Oxford Instruments Spectro-Mag II system and a Jasco J20 spectrometer which has had an absorption mode added. Absolute temperatures on this latter system should be good to ±0.3 K with temperature differences good to ±0.1 K. Cs_2NaYCl_6 was prepared by method E of Morss, et al.[12] Crystals were grown as previously described.[1a,b] Cr^{3+} was added as $Cs_2NaCrCl_6$ prepared in the same way. As the actual Cr^{3+} concentration of the samples was not known, all MCD and absorption values are in arbitrary units. However as the quantity of most interest, MCD/D, is independent of concentration, this proves to be no problem. These ratios should be good to ±20% except on the weakest transitions where errors as large as ±50% are possible. Peak energies are good